Nucleophilic Activation of Coordinated Carbon Monoxide. 3.[1] Hydroxide and Methoxide Reactions with the Trinuclear Clusters $M_3(CO)_{12}$ (M = Fe, Ru, or Os). Implications with Regard to Catalysis of the Water Gas Shift Reaction

David C. Gross and Peter C. Ford*

Contribution from the Department of Chemistry, University of California, Santa Barbara, California 93106. *Received June 4, 1984*

Abstract: Reported are quantitative investigations of the reactions of the triangular clusters $M_3(CO)_{12}$ (M = Fe, Ru, or Os) with methoxide ion in solution. In methanol under a CO atmosphere, both the osmium and ruthenium species form stable 1:1 methoxycarbonyl adducts ($M_3(CO)_{12} + NaOCH_3 \rightleftharpoons [M_3(CO)_{11}(CO_2CH_3)]Na$); however, for the triiron analogue this adduct undergoes fragmentation to give $Fe(CO)_4(CO_2CH_3)^-$. Initial adduct formation in each case occurs with an equilibrium constant of about 10^3 M^{-1}. In mixed tetrahydrofuran/methanol solutions, K_{eq} for $Ru_3(CO)_{11}(CO_2CH_3)^-$ is much larger, an indication of the greater activity of $NaOCH_3$ in the less protic solvent. Notably, in such solvent mixtures, the presence of excess methoxide also led to the formation of 2:1 adducts. Rates of adduct formation were examined by using stopped-flow kinetics techniques, and it was shown that in methanol the second-order rate constants (25 °C) are 11.3×10^3, 2.1×10^3, and 0.6×10^3 M^{-1} s^{-1} for $Fe_3(CO)_{12}$, $Ru_3(CO)_{12}$, and $Os_3(CO)_{12}$, respectively. Rates were much higher in the mixed THF/CH_3OH solutions; for example, k_1 (25 °C) for $Ru_3(CO)_{12}$ is 2.0×10^5 M^{-1} s^{-1} in 90/10 THF/CH_3OH (v/v). Monosubstitution of the ruthenium cluster with $(CH_3O)_3P$ markedly reduced the reactivity toward the anionic nucleophile. The reaction of the triruthenium species with hydroxide ($Ru_3(CO)_{12} + OH^- \rightleftharpoons Ru_3(CO)_{11}(CO_2H)^- \rightarrow HRu_3(CO)_{11}^- + CO_2$) was also investigated. Analysis of the reaction kinetics leads to the conclusion that formation of the initial hydroxycarbonyl adduct is somewhat less favorable and is slower than the analogous reaction of methoxide. The subsequent decarboxylation mechanism occurs by a base-independent pathway interpreted to be β-elimination with concerted transfer of the hydrogen to a metal center. These observations are discussed in terms of the water gas shift reaction and others catalyzed homogeneously by metal carbonyls.

Since 1977 when several independent communications described the homogeneous catalysis of the water gas shift reaction[2] (WGSR), there have been a number of reports describing such reactivity for a broad range of organometallic and coordination compounds.[3] Among the systems for which such catalytic activity has been described are the mono- and polynuclear carbonyls of the iron triad in alkaline solutions. For example, the first report of WGSR catalysis from this laboratory described the activity of solutions prepared from $Ru_3(CO)_{12}$ in alkaline aqueous ethoxyethanol. In this context a research interest of this laboratory has been the characterization of the mechanisms of key reactions in proposed catalytic cycles for the WGSR by such systems. The quantitative description of these mechanisms will provide an intellectual basis for the design of new or optimized catalysts for the shift reaction and other related processes.

For the shift reaction in mixed aqueous/organic solutions, a commonly postulated step is the reaction of hydroxide or water with coordinated CO to give a hydroxycarbonyl adduct, e.g.

$$M\text{-}CO + OH^- \rightarrow M\text{-}CO_2H^- \quad (1)$$

Subsequent decarboxylation would give the metal hydride ion

$$M\text{-}CO_2H^- \rightarrow M\text{-}H^- + CO_2 \quad (2)$$

The prototype of this conversion is eq 3, reported by Heiber and

$$Fe(CO)_5 + 2OH^- \rightarrow HFe(CO)_4^- + HCO_3^- \quad (3)$$

Leutert over 5 decades ago.[4] Nucleophilic activation of coordinated CO has further scope given that nucleophiles are employed as cocatalysts in a variety of metal carbonyl catalyzed reactions such as the reductive carbonylation of nitroaromatics, the reductions of CO, and the hydroformylation of olefins by CO/H_2O mixtures.[5] Despite this broad interest, there have been but a few detailed quantitative studies[6] of proposed steps of the catalysis mechanisms. The work described here is concerned with the characterization of the quantitative aspects of the reactions of the oxygen nucleophiles OH^- and CH_3O^- with the trinuclear carbonyls $Fe_3(CO)_{12}$, $Ru_3(CO)_{12}$, $Os_3(CO)_{12}$, and some derivatives. As noted, the ruthenium complex was used in one of the earlier WGSR homogeneous catalysts reported, and the chemistry of this and related ruthenium carbonyl species continues to hold considerable interest in other catalysis applications.[5b,c,g,7] Consequently, the decarboxylation step (eq 2) for this species was also examined quantitatively.

Experimental Section

Materials. Carbon monoxide (C.P. grade) and argon and nitrogen (Linde) were purified by being passed through a column of heated BASF Deox catalyst then a column of dried molecular sieve and Drierite. All solvents (reagent grade) were distilled under nitrogen or argon and outgassed prior to use. Tetrahydrofuran (THF) and diethyl ether were distilled from sodium benzophenone. Methanol, ethanol, and 2-propanol were distilled from CaH_2. Bis(triphenylphosphoranylidene)ammonium chloride, [PPN]Cl, was obtained from Aldrich and dried in vacuo at 100 °C for a minimum of 3 h prior to use. The ruthenium cluster $Ru_3(CO)_{12}$ was prepared as described previously via the high-pressure carbonylation of $RuCl_3$.[8] The substituted derivatives $Ru_3(CO)_{12-n}(P(OCH_3)_3)_n$ (n =

(1) (a) Part 2: Trautman, R. J.; Gross, D. C.; Ford, P. C., submitted for publication. (b) Taken in part from the Ph.D. Dissertation of D. C. Gross, UCSB, 1983.

(2) (a) Laine, R. M.; Rinker, R. G.; Ford, P. C. *J. Am. Chem. Soc.* **1977**, *99*, 252. (b) Cheng, C. H.; Hendersen, D. E.; Eisenberg, R. J. *J. Am. Chem. Soc.* **1977**, *99*, 2791. (c) Kang, H.; Mauldin, C.; Cole, T.; Sleigier, W.; Pettit, R. *J. Am. Chem. Soc.* **1977**, *99*, 8323.

(3) (a) Ford, P. C. *Acc. Chem. Res.* **1981**, *14*, 31 and references therein. (b) Halpern, J. *Comments Inorg. Chem.* **1981**, *1*, 1. (c) Eisenberg, R.; Hendricksen, D. E. *Adv. Catal.* **1979**, *28*, 79. (d) Laine, R.; in "Aspects of Homogenous Catalysis" Vol 5, R. Ugo, ed. pp 217-240; D. Reidel, London, 1984.

(4) (a) Hieber, W.; Leutart, F. *Z. Anorg. Allg. Chem.* **1932**, 145. (b) Trout, W. E. *J. Chem. Educ.* **1938**, *15*, 72.

(5) (a) von Kutepow, N.; Kindler, H. *Angew. Chem.* **1960**, *72*, 802. (b) Laine, R. M. *J. Am. Chem. Soc.* **1978**, *100*, 6451. (c) Alper, H.; Hashem, K. E. *J. Am. Chem. Soc.* **1981**, *103*, 6514. (d) Doxse, K. M.; Grubbs, R. H. *J. Am. Chem. Soc.* **1981**, *103*, 7696. (e) Casey, C. P.; Neumann, S. M. *J. Am. Chem. Soc.* **1976**, *98*, 5895. (f) Tain, W.; Wong, W.-K.; Gladysz, J. A. *J. Am. Chem. Soc.* **1979**, *101*, 1589. (g) Chen, M. J.; Feder, H. M.; Rathke, J. W. *J. Am. Chem. Soc.* **1982**, *104*, 7346.

(6) (a) Harkness, A. C.; Halpern, J. *J. Am. Chem. Soc.* **1961**, *83*, 1258. (b) Bercaw, J. E.; Goh, L.-V; Halpern, J. *J. Am. Chem. Soc.* **1972**, *94*, 6534. (c) Pearson, R. G.; Mauermann, H. *J. Am. Chem. Soc.* **1982**, *104*, 500. (d) Darensbourg, D. *Isr. J. Chem.* **1977**, *15*, 247.

(7) (a) Knifton, J.; Gigsby, R. A.; Fin, J. J. *Organometallics* **1984**, *3*, 62. (b) Darensbourg, D. J.; Pala, M.; Waller, J. *Organometallics* **1983**, *2*, 1285. (c) Dombek, B. D. *J. Am. Chem. Soc.* **1981**, *103*, 6508. (d) Fish, R. H.; Thormodsen, A. D.; Cremer, G. A. *J. Am. Chem. Soc.* **1982**, *104*, 5234.

0002-7863/85/1507-0585$01.50/0

1, 2, or 3) were prepared by procedures reported by Bruce and coworkers[9] as follows. An anhydrous THF solution of $Ru_3(CO)_{12}$ (100 mg, 0.156 mmol) and the stoichiometrically required amount of $P(OCH_3)_3$ was treated with about 5 drops of sodium diphenylketal solution (from the bottom of a THF still) and allowed to react at room temperature for a period ranging from 5 min for the preparation of $Ru_3(CO)_{11}(P(OCH_3)_3)$ to 30 min for $Ru_3(CO)_9(P(OCH_3)_3)_3$. Workup involved removing the solvent in vacuo, dissolving the residue in a minimum of hexane, and chromatographing this solution on a silica gel column with hexane as eluent. The ruthenium clusters eluted in the order of increasing extent of substitution. The aliquots containing the various bands were collected, and the products isolated by evaporative removal of the solvent from the various fractions then were recrystallized from hot hexane. Yields of the desired products averaged 60%.

The iron and osmium trinuclear clusters $Fe_3(CO)_{12}$ and $Os_3(CO)_{12}$ were purchased from Aldrich Chemicals and Strem Chemicals, respectively, and used as supplied.

The group 1A methoxides ($M'OCH_3$, M' = Na, Li, K) were prepared as methanolic solutions. Small samples of the metals were cleaned with hexane, shaved with a razor blade to approximately 1 cm^3, washed with 2-propanol, and then immediately added against a countercurrent of Ar to a Schlenk flask containing stirring anhydrous CH_3OH (about 50 mL) cooled to 0 °C. After completion of the reaction, the solutions were degassed by several freeze–pump–thaw cycles and stored under Ar. Methoxide concentration was determined by titration against standardized aqueous HCl solutions with phenolphthalein or bromothymol blue as an indicator. Sodium isopropoxide in 2-propanol was prepared and standardized by analogous procedures. The tetra(*n*-butyl)ammonium bases $[(n\text{-}Bu)_4N]OH$ and $[(n\text{-}Bu)_4N]OCH_3$ were prepared from solutions of the former purchased from Aldrich as a 1 M solution in CH_3OH or as a 40% by wt solution in H_2O. The methoxide was prepared by vacuum removal of all volatiles at 40 °C from either solution (about 10 mL) in a Schlenk flask. The resulting clear oil was taken up in anhydrous degassed CH_3OH, titrated against standardized aqueous HCl solution, and stored under Argon.

Instrumentation. Infrared spectra were obtained on a Perkin-Elmer 683 spectrophotometer. Liquid samples were placed between NaCl or IR Trans plates separated by Teflon spacers (0.015 to 0.20 mm). Solid samples were run either as KBr pellets (1/100, w/w sample/KBr) or as Nujol mulls. UV–vis spectra were run on a Cary 14 or 118 recording spectrophotometer in quartz cells of path length 0.1 cm (Hellma) or 1.0 cm (Precision). ^1H NMR spectra were obtained on a Varian Associates XL-100 or a Nicolet 300-MHz NMR spectrometer operating in the pulsed Fourier transform mode with deuterium lock. An internal lock was achieved with deuterated solvents; samples were referenced to the residual protons in that solvent.

Kinetics and Equilibrium Studies. Rates of nucleophilic addition were determined with a Durrum-Gibson D110 stopped-flow spectrophotometer. In a determination, a neutral metal carbonyl solution ($\sim 10^{-4}$ M) was combined with alkoxide or hydroxide solutions of the identical solvent composition. The hardware surrounding the solutions, the drive syringes and observation block, were thermostated to ±0.1 °C with a Haake FS-2 circulator bath. Solutions were temperature equilibrated for 15 min before analysis, and all solutions were prepared and transferred to the spectrometer under deaerated conditions with N_2 or CO as the blanketing gas (normally CO). In early studies the data from a rate determination, in the form of absorbance vs. time traces, were recorded on a Tektronix F103 storage oscilloscope triggered by the stop syringe of the stopped-flow spectrophotometer. This trace was then photographed with a Tektronix C-5B oscilloscope camera, digitized, and stored in data files on the PDP-11/34 computer. In latter experiments the temporal absorbance output from the stopped-flow spectrophotometer was recorded with a Biomation 805 waveform recorder and then transferred digitally to a Hewlett-Packard 86 microcomputer for mathematical analysis.

The rates of nucleophilic addition to the neutral metal carbonyls (eq 4) were determined under conditions where the nucleophilic concentration greatly exceeded those of the carbonyl substrates. Under these circum-

$$M_3(CO)_{12} + OR^- = M_3(CO)_{11}(CO_2R)^- \quad (4)$$

stances, plots of ln (abs(t) − abs(∞)) vs. time were typically linear (correlation coefficient >0.998) for more than 3 half-lives. Linear plots indicated the reaction to be first order in metal carbonyl concentration.

$$-\frac{d}{dt}[M_3(CO)_{12}] = k_{obsd}[M_3(CO)_{12}] \quad (5)$$

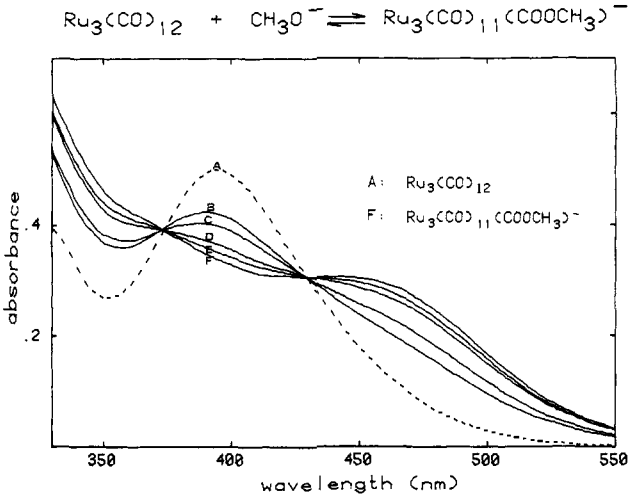

Figure 1. Spectral changes observed when $NaOCH_3$ is added to $Ru_3(CO)_{12}$ in methanol: $[NaOCH_3]$ = 0.00 M (A), 7.4×10^{-4} M (B), 1.45×10^{-3} M (C), 5.2×10^{-3} M (D), 0.11 M (E), 0.22 M (F).

First-order rate constants k_{obsd} were also determined by the kinetic over-relaxation method of Swain et al.[10]

Values of the observed rate constants, k_{obsd}, were obtained over as wide a range of $[OR^-]$ as possible. The limiting factor at high $[OR^-]$ was the dead time (~2 ms) of the stopped-flow spectrophotometer. The limiting factor at low $[OR^-]$ was the need to maintain a 10-fold excess over $[M_3(CO)_{12}]$ in order to maintain first-order kinetics. Plots of k_{obsd} vs. $[OR^-]$ were linear, indicating the rate of adduct formation to be first order in $[OR^-]$ (see Results).

The rates of $HRu_3(CO)_{11}^-$ formation in alkaline aqueous methanol solutions were of a time scale that the reaction could be followed by monitoring electronic spectral changes with a Cary 14 recording spectrophotometer. A special quartz spectrometer cell was constructed so that the solutions could be introduced via syringe techniques and the cell subsequently pressurized with CO/argon mixtures to a total pressure of several atmospheres.

The stability of $Ru_3(CO)_{11}(CO_2CH_3)^-$ and of $Os_3(CO)_{11}(CO_2CH_3)^-$ in anhydrous THF or CH_3OH allowed the equilibrium constant for methoxycarbonyl adduct formation to be determined by a static spectroscopic technique. At high $NaOCH_3$ concentrations effectively all the carbonyl complex was found as the methoxide adduct and the electronic spectrum of this species was obtained from such solutions. At intermediate methoxide concentrations, both $M_3(CO)_{12}$ and $M_3(CO)_{11}(CO_2CH_3)^-$ were present, and the concentratons of each could be quantitatively evaluated from the absorbance spectrum and K_{eq} determined from eq 6.

$$K_{eq} = \frac{[M_3(CO)_{11}(CO_2CH_3)^-]}{[M_3(CO)_{12}][OCH_3^-]} \quad (6)$$

Results

I. Characterization of Reactions with Methoxide. $Ru_3(CO)_{12}$. Methanol solutions of $Ru_3(CO)_{12}$ under CO (P_{CO} = 1.0 atm) display a strong absorption band in the electronic spectrum at λ_{max} 392 nm (ϵ 6.9×10^3 M^{-1} cm^{-1}) plus a minimum at 350 nm (ϵ 3.45×10^3). Sequential addition of $NaOCH_3$ led to the spectral changes shown in Figure 1 with new absorption appearing at 460 and 360 nm and isosbestic points maintained at 428 and 394 nm. At the higher concentration of $NaOCH_3$, a limiting spectrum with λ_{max} 460 nm (ϵ 4.0×10^3) and 360 nm (shoulder, ϵ 5.8×10^3) was obtained. Dropwise addition of CF_3CO_2H to such solution led to the immediate reversal of these spectral changes to regenerate the original spectrum of $Ru_3(CO)_{12}$. Thus, it was concluded that CH_3O^- reversibly forms a stable one-to-one adduct with $Ru_3(CO)_{12}$ in methanol, e.g.

$$Ru_3(CO)_{12} + CH_3O^- \underset{}{\overset{K_{eq}}{\rightleftharpoons}} \underset{A}{Ru_3(CO)_{11}(CO_2CH_3)^-} \quad (7)$$

The equilibrium constant was determined from the spectral

(8) Eady, C. R.; Jackson, P. F.; Johnson, B. F. G.; Lewis, J.; Malatesta, M. C.; McPartlin, M.; Nelson, W. J. H. *J. Chem. Soc. Dalton Trans.* **1980**, 383.

(9) Bruce, M. I.; Kehoe, D. C.; Matisons, J. G.; Nicholson, B. K.; Rieger, P. H.; Williams, M. L. *J. Chem. Soc., Chem. Commun.* **1982**, 442.

(10) Swain, C. G.; Swain, M. S.; Berg, L. F. *J. Chem. Inf. Comput. Sci.* **1980**, *20*, 47.

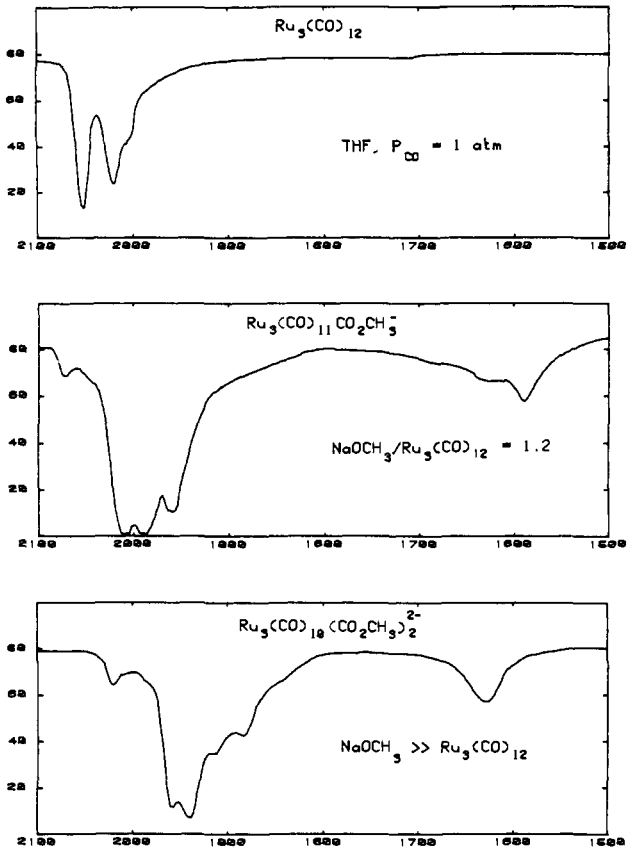

Figure 2. IR spectra in THF of $Ru_3(CO)_{12}$, $Na[Ru_3(CO)_{11}(CO_2CH_3)]$, and $Na_2[Ru_3(CO)_{10}(CO_2CH_3)_2]$.

changes at 490 nm where the absorbance differences between $Ru_3(CO)_{12}$ and the adduct are the largest (2.3×10^3 M^{-1} cm^{-1}). For seven $NaOCH_3$ concentrations over the range (0.7 to 5.2) $\times 10^{-3}$ M, K_{eq} was found to have the value $(1.19 \pm 0.14) \times 10^3$ M^{-1} (23 °C).

The proposal that A is the methoxycarbonyl complex was substantiated by IR spectral experiments. In methanol $Ru_3(CO)_{12}$ displays ν_{CO} bands at 2061 s, 2031 m and 2011 w cm^{-1}. Addition of 0.1 M $NaOCH_3$ to 5×10^{-3} M $Ru_3(CO)_{12}$ in methanol gave an entirely different spectrum with ν_{CO} bands at 2074 w, 2022 s, 2001 s, 1972 m, and 1610 w cm^{-1} (Figure 2). The lower ν_{CO} values of the latter species are consistent with the negative charge of the adduct, and the 1610-cm^{-1} value is about that expected for the coordinated $-CO_2CH_3$ group.[11,12] In a separate study, Anstock has isolated the PPN^+ salt of $Ru_3(CO)_{11}(CO_2CH_3)^-$ and characterized this by chemical analysis and ^{13}C and ^1H NMR.[13]

Addition of a slight molar excess of $NaOCH_3$ to CO-saturated THF solutions of $Ru_3(CO)_{12}$ resulted in solutions displaying electronic and infrared spectral properties consistent with the formation of A. However, in this solvent the IR spectrum proved quite dependent on the countercation. The Na^+ salt displayed a ν_{CO} band for the methoxycarbonyl group at 1595 cm^{-1} (about 15 cm^{-1} lower frequency than in methanol), but the PPN^+ and $(n\text{-}Bu)_4N^+$ salts both showed this band at higher frequency (1640 cm^{-1}). For the latter salts the terminal CO's were shifted to slightly lower frequency than that found for the Na^+ salt. This behavior is consistent with that seen for the mononuclear adducts $M(CO)_4(CO_2CH_3)^-$ where the differences between the IR spectra of the Na^+ and PPN^+ salts were attributed to specific interaction between the hard Na^+ and the oxygen of the methoxycarbonyl group.[1a]

In contrast to the behavior in methanol, the addition of excess $NaOCH_3$ (0.014 M) to a 90/10 THF/CH_3OH solution of $Na[Ru_3(CO)_{11}(CO_2CH_3)]$ (prepared from 0.0045 M $NaOCH_3$ plus 0.0039 M $Ru_3(CO)_{12}$ under CO (1.0 atm)) led to a decrease in IR bands attributed to A and to the appearance of the bands (Figure 2) of a new metal carbonyl complex (B). The same species was formed by the reaction of $Ru_3(CO)_{12}$ in CO saturated THF with a suspension of $NaOCH_3$ and from the reaction of excess $[(n\text{-}Bu)_4N]OCH_3$ with $Ru_3(CO)_{12}$ in THF under CO. In both cases A was formed first. The second case was followed by electronic spectra changes, and isosbestic points were maintained at 574 and 427 nm during the slow conversion of A to B. These observations suggest that B is a bis(methoxycarbonyl) species, e.g.

$$Ru_3(CO)_{11}(CO_2CH_3)^- + CH_3O^- \rightarrow Ru_3(CO)_{10}(CO_2CH_3)_2^{2-} \quad (8)$$

A somewhat different situation was encountered if solutions of A in CO-saturated 90/10 THF/CH_3OH were flushed with argon. A third species C displaying IR bands at 2064 w, 2014 s, 1998 s, 1986 vs, 1951 sh, 1941 s, 1793 s, an 1735 w cm^{-1} was observed. The same species was directly formed from $Ru_3(CO)_{12}$ plus $NaOCH_3$ in THF under argon. The infrared spectrum of C is quite close to that of the $Ru_3(CO)_{10}(\mu\text{-}CON(CH_3)_2)^-$ ion characterized previously by Kaesz and co-workers.[14] Thus, we propose that C has an analogous structure with the methoxycarbonyl group bridging two ruthenium atoms as a bidentate ligand and each metal–metal bond also bridged by a carbonyl. This species would be formed by CO dissociation from A followed by coordination of the methoxycarbonyl oxygen and associated rearrangements

$$Ru_3(CO)_{11}(CO_2CH_3)^- \xrightarrow{-CO} Ru_3(CO)_{10}(CO_2CH_3)^- + CO \rightarrow Ru_3(CO)_{10}(\mu\text{-}CO_2CH_3)^- \quad (9)$$

A similar transformation was seen for the bis(methoxycarbonyl) species B. When a THF solution of this adduct (Na^+ salt) was flushed with argon to remove the CO, a new infrared spectrum with ν_{CO}(terminal) bands at 2030 w, 2019 m, 1967 vs, 1930 s and 1907 m cm^{-1}, ν_{CO}(bridging) bands at 1791 s and 1742 m cm^{-1}, and ν_{CO}(methoxycarbonyl) at 1657 m, br cm^{-1} was observed.

$Ru_3(CO)_{12-n}(P(OCH_3)_3)_n$ (n = 1–3). No noticable electronic spectral changes were seen when excess $NaOCH_3$ was added to methanol solutions of $Ru_3(CO)_{11}(P(OCH_3)_3)$. However, in the more active medium 90/10 (v/v) THF/CH_3OH, addition of methoxide to this cluster led to a sharp color change from yellow to deep red and a shift in the λ_{max} of the predominant visible absorption band from 404 nm (7.8×10^3) to 452 nm (5.6×10^3). The resulting IR spectrum displayed a ν_{CO} band (1592m cm^{-1}) characteristic of a methoxycarbonyl ligand. Under similar conditions (94/6 THF/CH_3OH, 0.06 mM $NaOCH_3$) there was no observable change in the electronic spectra of either the disubstituted cluster $Ru_3(CO)_{10}(P(OCH_3)_3)_2$ or the trisubstituted cluster $Ru_3(CO)_9(P(OCH_3)_3)_3$.

$Os_3(CO)_{12}$. Sequential addition of $NaOCH_3$ to methanol solutions of $Os_3(CO)_{12}$ under CO (1 atm) led to disappearance of the electronic absorption bands of $Os_3(CO)_{12}$ (λ_{max} 328 nm (9.6×10^3) and 383 nm (sh, 3.3×10^3)) and the appearance of new bands at 413 nm (3.6×10^3) and 340 nm (sh, 7.2×10^3) with isosbestic paints maintained at 345 and 386 nm. At high methoxide concentrations, a limiting spectrum was obtained, indicating the formation of a stable 1:1 adduct (eq 10). The IR spectrum of the adduct in 50/50 THF/CH_3OH (Table I) shows a band at 1595 cm^{-1} consistent with the presence of a CO_2CH_3 group

$$Os_3(CO)_{12} + CH_3O^- \rightarrow Os_3(CO)_{11}(CO_2CH_3)^- \quad (10)$$

The equilibrium constant for eq 10 was determined from spectral data at 430 cm where the extinction coefficients of $Os_3(CO)_{12}$ and $Os_3(CO)_{11}(CO_2CH_3)^-$ are 770 and 2.8×10^3 M^{-1} cm^{-1}, respectively. Over the $[NaOCH_3]$ range 4.4×10^{-4} to 3.4×10^{-2} M, the K_{eq}(static) value was determined to be 690 ± 17 M^{-1}.

$Fe_3(CO)_{12}$. A somewhat different situation was found for the iron cluster $Fe_3(CO)_{12}$. Addition of methanolic $NaOCH_3$ to methanol solutions of $Fe_3(CO)_{12}$ under CO (P_{CO} = 1 atm) leads to the UV–vis spectral changes seen in Figure 3. The $Fe_3(CO)_{12}$ absorption bands at 602 and 430 nm (sh) were immediately shifted to give new bands at 615 and 415 nm (sh). Subsequently, over a period of minutes these bands faded to give a spectrum devoid of visible absorbances. The IR spectra of similar solutions prepared

Table I. IR Spectral Properties of Key Trimetallic Clusters and Their Methoxycarbonyl Adducts

cluster	ν_{CO} bands (in cm^{-1})
$Ru_3(CO)_{12}$[a]	2061 s, 2031 m, 2011 w
$Na[Ru_3(CO)_{11}(CO_2CH_3)]$[a]	2074 w, 2022 s, 2001 s, 1972 m, 1610 w
$Na[Ru_3(CO)_{11}(CO_2CH_3)]$[b]	2074 w, 2015 s, 1997 s, 1967 m, 1635 vw, 1595 w
$[PPN][Ru_3(CO)_{11}(CO_2CH_3)]$[c]	2072 w, 2014 s, 1995 s, 1964 m, 1640 m
$[PPN][Ru_3(CO)_{10}(\mu\text{-}CO_2CH_3)]$[c]	2064 w, 2014 s, 1998 s, 1986 vs, 1951 sh, 1941 s, 1793 s, 1735 w
$[Na]_2[Ru_3(CO)_{10}(CO_2CH_3)_2]$[b]	2030 w, 1965 s, 1947 vs, 1922 m, 1893 m, 1637 m
$Ru_3(CO)_{11}(P(OCH_3)_3)$[c]	2102 m, 2050 vs, 2035 s, 2019 vs, 2000 m, 1994 m, 1984 w, 1967 w
$Na[Ru_3(CO)_{10}(P(OCH_3)_3)(CO_2CH_3)]$[b]	2064 m, 2002 s, 1984 s, 1952 m, 1592 m
$Os_3(CO)_{12}$[c]	2065 s, 2031 m, 2009 w, 1999 w
$Na[Os_3(CO)_{11}(CO_2CH_3)]$[b]	2050 vw, 2027 s, 2019 sh, 2001 vs, 1967 m, 1950 m, 1595 m
$Fe_3(CO)_{12}$[c]	2045 s, 2019 m, 1865 w, 1825 w
$Na[Fe_3(CO)_{11}(CO_2CH_3)]$[d]	2023 w, 1933 sh, 1917 s, 1585 m

[a] In methanol. [b] In 95/5 (v/v) THF/CH_3OH. [c] In THF. [d] Spectrum of $Fe_3(CO)_{12}$ in 95/5 THF/CH_3OH 2 min after excess $NaOCH_3$ is added to the solution.

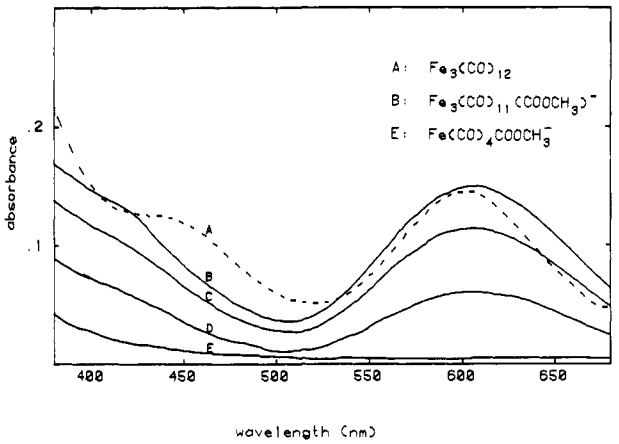

Figure 3. Electronic spectral changes effected by the addition of $NaOCH_3$ to $Fe_3(CO)_{12}$ in methanol solution under carbon monoxide (P_{CO} = 1 atm). B is the spectrum immediately after mixing. C, D, and E are spectra taken chronologically over a few minutes elapsed time.

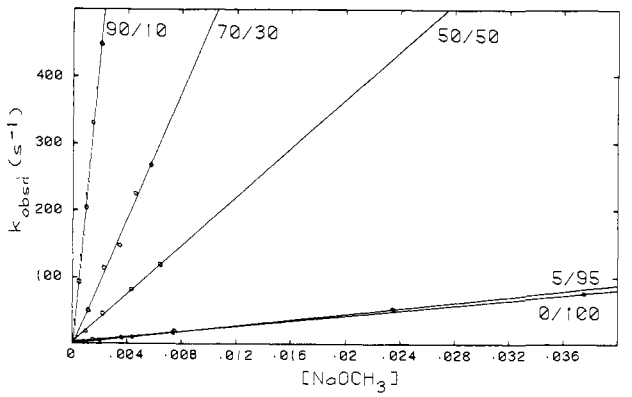

Figure 4. Plots of k_{obsd} vs. [$NaOCH_3$] for the reaction of $NaOCH_3$ plus $Ru_3(CO)_{12}$ in different mixed (v/v) THF/CH_3OH solvents at 25 °C.

by addition of excess $NaOCH_3$ (0.033 M) to $Fe_3(CO)_{12}$ (0.0035 M) in 94/6 THF/CH_3OH under CO proved more diagnostic. The initial spectrum after mixing gave a number of ν_{CO} bands, and those at 2023 w, 1933 sh, 1917 s, and 1585 m cm^{-1} were attributable to the presence of the colorless mononuclear iron complex $Fe(CO)_4(CO_2CH_3)^-$ reported previously.[1a] The remaining bands at 2009 s, 1993 s, and 1970 m cm^{-1} were consistent with the terminal ν_{CO} bands expected for an anionic cluster, e.g., the methoxycarbonyl adduct. These latter bands disappeared in a few minutes to give the spectrum of $Fe(CO)_4(CO_2CH_3)^-$ only. Since the intermediate species displayed an electronic spectrum similar to the starting complex, a logical interpretation of these results is the following sequence

$$Fe_3(CO)_{12} + CH_3O^- \rightleftharpoons Fe_3(CO)_{11}(CO_2CH_3)^- \quad (11)$$

$$Fe_3(CO)_{11}(CO_2CH_3)^- + 3CO + 2CH_3O^- \rightarrow\rightarrow 3Fe(CO)_4(CO_2CH_3)^- \quad (12)$$

II. Kinetics of Methoxycarbonyl Adduct Formation in CH_3OH. $Ru_3(CO)_{12}$. Rates of reaction between methoxide and $Ru_3(CO)_{12}$ were measured with stopped-flow techniques to follow absorbance changes at 490 nm. Under conditions of excess base, first-order kinetics behavior was observed in each case (eq 5), and a plot of the resulting k_{obsd} values vs. [$NaOCH_3$] was linear with small non-zero intercepts (Figure 4). This behavior is consistent with that expected for relaxation to an equilibrium mixture, e.g.

$$M_3(CO)_{12} + OR^- \underset{k_{-1}}{\overset{k_1}{\rightleftharpoons}} M_3(CO)_{11}(CO_2R)^- \quad (13)$$

where

$$k_{obsd} = k_1[OR^-] + k_{-1} \quad (14)$$

and

$$K_{eq} = k_1/k_{-1} \quad (15)$$

The slope is the second-order rate constant k_1; the intercept is k_{-1}. In 25 °C methanol, the values of k_1, k_{-1}, and K_{eq} determined in this manner for $Ru_3(CO)_{12}$ were (2.05 ± 0.16) × 10^3 M^{-1} s^{-1}, 2.1 ± 1.1 s^{-1}, and (approximately) 1 × 10^3 M^{-1}, respectively. The K_{eq}(kinetic) determined from these data was close to that determined above by static spectral measurements (1.2 × 10^3 M^{-1}); however, the former value is burdened with large uncertainties owing to the uncertainties in the extrapolated k_{-1} value.

For the reaction of $Ru_3(CO)_{12}$ with other methoxides, plots similar to Figure 4 were obtained for $LiOCH_3$ and $[(n\text{-}Bu)_4]OCH_3$ in methanol. The k_1 for $LiOCH_3$, (2.13 ± 0.04) × 10^3 M^{-1} s^{-1}, was within experimental uncertainty to that measured for $NaOCH_3$; however, the value measured for $[(n\text{-}Bu)_4]OCH_3$ was somewhat larger, (2.37 ± 0.04) × 10^3 M^{-1} s^{-1} at 25 °C.

$Os_3(CO)_{12}$ and $Fe_3(CO)_{12}$. The formation kinetics of the stable methoxycarbonyl adduct of $Os_3(CO)_{12}$ (eq 8) and of the transient adduct of $Fe_3(CO)_{12}$ (eq 11) were also studied by the stopped-flow technique. Plots of the observed first-order rate constants k_{obsd} measured at 430 nm for $Os_3(CO)_{12}$ and at 650 nm for $Fe_3(CO)_{12}$ vs. [$NaOCH_3$] were linear with nonzero intercepts. The resulting k_{obsd} and k_{-1} values are summarized in Table II as are the K_{eq}(kinetic) values determined from the k_1/k_{-1} ratios. As noted above the latter values suffer rather large uncertainties.

III. Kinetics of Alkoxycarbonyl Adduct Formation in Other Solvents. $Ru_3(CO)_{12}$ in THF/CH_3OH. Rates for the formation of A were also measured in mixed THF/CH_3OH solvents. Plots of k_{obsd} vs. [$NaOCH_3$] were markedly dependent on the solvent composition (Figure 4), giving much larger k_1 and K_{eq}(kinetic) values with increasing THF composition (Table III). A determination of the equilibrium constant for eq 7 from the spectral differences in solution gave a K_{eq}(static) value of (1.64 ± 0.15) × 10^3 M^{-1} in 5/95 THF/CH_3OH, within experimental uncertainty of the K_{eq}(kinetic) value measured for this system (Table III).

$Ru_3(CO)_{11}(P(OCH_3)_3)$ in THF/CH_3OH. Substitution of a single phosphite onto the triruthenium cluster reduced the reactivity with $NaOCH_3$ dramatically. Rates measured both in 90/10 THF/CH_3OH and in 50/50 THF/CH_3OH showed the forward rate constant k_1 roughly two orders of magnitude smaller

Table II. Rate Constants for the Reactions of $M_3(CO)_{12}$ with Sodium Methoxide in Methanol[a]

$$M_3(CO)_{12} + CH_3O^- \underset{k_{-1}}{\overset{k_1}{\rightleftharpoons}} M_3(CO)_{11}(CO_2CH_3)^-$$

complex	k_1 (in 10^3 M^{-1} s^{-1})	k_{-1} (in s^{-1})	K_{eq}(kinetic)[b] (in 10^3 M^{-1})	K_{eq}(static)[c] (in 10^3 M^{-1})
$Fe_3(CO)_{12}$	11.3 ± 0.7	8.1 ± 3.5	1.4 ± 0.6	
$Ru_3(CO)_{12}$	2.05 ± 0.16	2.1 ± 1.1	1.0 ± 0.5	1.19 ± 0.13
$Os_3(CO)_{12}$	0.61 ± 0.04	0.75 ± 0.24	0.8 ± 0.3	0.69 ± 0.02
$Fe(CO)_5$[d]	1.1	165	0.007	0.006
$Fe(CO)_5$[d,e]	1.8	135	0.013	0.015
$Ru(CO)_5$[d,e]	7	85	0.1	0.11
$Os(CO)_5$[d,f]	14			

[a] 25 °C, P_{CO} = 1 atm. [b] K_{eq}(kinetic) = k_1/k_{-1}. [c] Determined from static spectral measurements. [d] Reference 1a. [e] 10/90 (v/v) THF/CH_3OH. [f] 5/95 (v/v) THF/CH_3OH.

Table III. Rate Constants for the Reaction of $Ru_3(CO)_{12-n}L_n$ with Alkoxide in Various Solvent Mixtures[a]

$$Ru_3(CO)_{12-n}L_n + RO^- \underset{k_{-1}}{\overset{k_1}{\rightleftharpoons}} Ru_3(CO)_{11-n}L_n(CO_2R)^-$$

complex	solvent	k_1 (in 10^3 M^{-1} s^{-1})	k_{-1} (in s^{-1})	K_{eq}(kinetic) (in 10^3 M^{-1})
$Ru_3(CO)_{12}$	CH_3OH	2.05 ± 0.16	2.1 ± 1.1	~1.0
	5/95 THF/CH_3OH	2.20 ± 0.01	1.1 ± 0.1	1.9
	50/50 THF/CH_3OH	18.0 ± 0.7	3.3 ± 2.6	~5
	70/30 THF/CH_3OH	47.0 ± 3.0	1 ± 5	
	90/10 THF/CH_3OH	204 ± 13	6.9 ± 2.3	30
$Ru_3(CO)_{11}(P(OCH_3)_3)$	50/50 THF/CH_3OH	0.20 ± 0.04	9.1 ± 1.3	~0.02
	90/10 THF/CH_3OH	3.46 ± 0.16	1.7 ± 1	~2
$Ru_3(CO)_{12}$	90/10 THF/H_2O[b]	12.9 ± 0.6	8.2 ± 5.2	~1.5
	87.5/12.5 THF/H_2O	12.2 ± 1	4.4 ± 3.2	~3

[a] 25 °C, P_{CO} = 1 atm, base added as $NaOCH_3$ except where noted, L = $P(OCH_3)_3$. [b] Base added as $[(n\text{-}Bu)_4N]OH$. [c] Base added as KOH.

than the analogous rate constant measured for $Ru_3(CO)_{12}$ under the same conditions (Table III). In contrast, the k_{-1} values appear to be much less affected.

$Ru_3(CO)_{12}$ in Isopropyl Alcohol. This solvent system was chosen in order to examine the reactivities of several different oxygen nucleophiles RO^- under very similar conditions. The K_e values (eq 16) determined for CH_3OH, H_2O, and C_2H_5OH are 4.00, 1.20, and 0.95 M^{-1}, respectively.[15]

$$ROH + i\text{-}PrO^- \rightleftharpoons RO^- + i\text{-}PrOH \qquad (16)$$

$$K_e = [RO^-]/[ROH][i\text{-}PrO^-]$$

Hence, in isopropyl alcohol solutions, the concentration of RO^- can be expressed as

$$[RO^-] = \frac{K_e[ROH][base]}{1 + K_e[ROH]} \qquad (17)$$

where [base] = $[RO^-]$ + $[i\text{-}PrO^-]$. In the presence of a relatively small conncentration of ROH (5–10%), the base will be present principally as RO^-, so it was possible to compare the reactivities of the four anions OH^-, CH_3O^-, $C_2H_5O^-$, and $i\text{-}PrO^-$ for a set of closely analogous conditions. Formation of the isopropoxy

$$Ru_3(CO)_{12} + RO^- \underset{k_{-1}}{\overset{k_1}{\rightleftharpoons}} Ru_3(CO)_{11}(CO_2R)^- \qquad (18)$$

adduct (eq. 18, RO^- = $i\text{-}PrO^-$) in isopropyl alcohol solution was followed by monitoring temporal absorbance changes at 490 nm in the stopped-flow spectrophotometer. Plots of k_{obsd} vs. $[i\text{-}PrO^-]$ were linear over the range 0.002 to 0.02 M, giving the k_1 value of (3.7 ± 0.1) × 10^3 M^{-1} s^{-1}. Similar studies carried out in the mixed solvents (e.g., in 5/95 (v/v) $H_2O/i\text{-}PrOH$ where the base is 77% OH^-) gave k_{obsd} values representing the composite reactivities of the two nucleophiles present, i.e., k_{obsd} = $k_1'[RO^-]$ + $k_1[i\text{-}PrO^-]$. Plots of k_{obsd} vs. total [base] were linear, giving the slopes reported in Table IV. From these values and eq 17 were calculated the second-order rate constants for the individual RO^- ions. Notably, the order of RO^- reactivity, CH_3O^- > OH^- > $C_2H_5O^-$, is inverted from the relative Brønsted basicities of these anions in isopropyl alcohol.

Table IV. Rates of the Reaction of Various RO^- Nucleophiles with $Ru_3(CO)_{12}$ in Isopropyl Alcohol/ROH Solutions[a]

$Ru_3(CO)_{12}$ + RO^- (or $i\text{-}PrO^-$) ⇌ $Ru_3(CO)_{11}(CO_2R)^-$ (or $Ru_3(CO)_{11}(CO_2\text{-}i\text{-}Pr)^-$)

$k_{obsd} = k_1'[RO^-] + k_1[i\text{-}PrO^-] = k_s$[base] ([base] = $[RO^-] + [i\text{-}PrO^-]$)

solvent	k_s (in 10^3 M^{-1} s^{-1})	RO^-	k_1'[b] (in 10^3 M^{-1} s^{-1})
10/90 (v/v) $CH_3OH/i\text{-}PrOH$	18.0 ± 1.0	CH_3O^-	16.6 ± 0.9
5/90 (v/v) $H_2O/i\text{-}PrOH$	8.9 ± 0.9	OH^-	8.0 ± 1.5
10/90 (v/v) $EtOH/i\text{-}PrOH$	7.1 ± 0.2	EtO^-	5.8 ± 02
100% $i\text{-}PrOH$	3.7 ± 0.1	$i\text{-}PrO^-$	3.7 ± 0.1

[a] 25 °C, P_{CO} = 1.0 atm, base was added as $[i\text{-}PrO]Na$. [b] Analyzed according to ref 16.

IV. Characterization of Reactions with Hydroxide. $Ru_3(CO)_{12}$ and $Ru_3(CO)_{12-n}(P(OCH_3)_3)_n$. Addition of KOH to $Ru_3(CO)_{12}$ in 5/95 H_2O/THF under CO (1 atm) led to the immediate formation of a new species D displaying an electronic spectrum (shoulder at 460 nm) reminiscent of that of $Ru_3(CO)_{11}(CO_2CH_3)^-$. By analogy this is proposed to be the hydroxycarbonyl analogue

$$Ru_3(CO)_{12} + OH^- \underset{k_{-2}}{\overset{k_2}{\rightleftharpoons}} Ru_3(CO)_{11}(CO_2H)^- \qquad (19)$$

Whereas the methoxycarbonyl adduct under CO proved stable, D underwent a slow subsequent reaction to give the known species $HRu_3(CO)_{11}^-$ (λ_{max} 385 nm, ϵ 7.2 × 10^3 M^{-1} cm^{-1}) with isosbestic points at 410 and 370 nm maintained during the course of the reaction (Figure 5). Similar reactions were noted when $[(n\text{-}Bu_4)_4N]OH$ or [(Crypt-222)K]OH were added to $Ru_3(CO)_{12}$ in aqueous THF; however, for the former base, reaction with a large stoichiometric excess of base led to the formation of uncharac-

(11) Petz, W. *J. Organomet. Chem.* **1976**, *105*, C19.
(12) Garlaschelli, L.; Martinengro, S.; Chini, P.; Canziani, F.; Bau, R. *J. Organomet. Chem.* **1981**, *213*, 379.
(13) Anstock, M.; Taube, D.; Gross, D. C.; Ford, P. C., to be submitted.
(14) Kaesz, H. D.; Lin, Y. C.; Boag, N. M.; Mayer, A. *Inorg. Chem.* **1982**, *21*, 1706.
(15) Hine, J.; Hine, M. *J. Am. Chem. Soc.* **1952**, *74*, 3266.

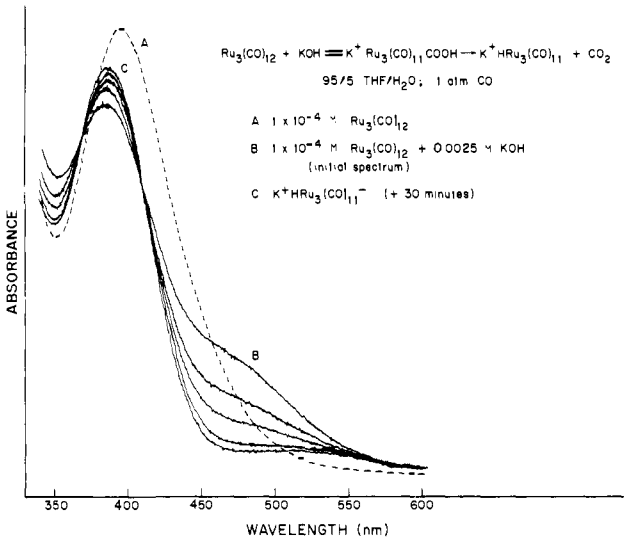

Figure 5. Spectral changes resulting from the addition of KOH in H_2O to $Ru_3(CO)_{12}$ in THF. Spectrum A: $Ru_3(CO)_{12}$ in THF. Spectrum B: Initial spectrum after mixing $Ru_3(CO)_{12}$ and KOH in 5/90 v/v H_2O/THF. Spectrum C: Spectrum of solution B after 30 min of reaction at ambient temperature. (This spectrum agrees with that of $HRu_3(CO)_{11}^-$.)

terized metal carbonyls believed to be higher order clusters.[8] The $HRu_3(CO)_{11}^-$ ion also forms from the reaction of $Ru_3(CO)_{12}$ with base in aqueous methanol.[16]

Although no spectral changes were seen when $NaOCH_3$ was added to a solution of $Ru_3(CO)_{11}(P(OCH_3)_3)$ in methanol (see above), addition of water to the resulting solution did lead to subsequent reaction. Over 30 min, there was a slow disappearance of the initial cluster's absorption band at λ_{max} 404 nm with the corresponding appearance of a new band at λ_{max} 396 nm (7.9×10^3 M^{-1} cm^{-1}) with isosbestic points maintained at 515 and 407 nm. When the reaction was complete, the solvent was removed in vacuo and the remaining red oil was dissolved in acetone-d_6. The ^1H NMR spectrum displayed a doublet in the hydride region (δ −12.39, J_{PH} = 6.9 Hz) and the IR spectrum listed in Table I. The same spectral properties were observed for the product of the reaction of $HRu_3(CO)_{11}^-$ with 1 equiv of $P(OCH_3)_3$.[17] Thus, we conclude that these spectral changes represent the following transformation

$$Ru_3(CO)_{11}(P(OCH_3)_3) + OH^- \rightarrow HRu_3(CO)_{10}(P(OCH_3)_3)^- + CO_2 \quad (20)$$

Notably, the formation of the hydride anion occurs without any measurable buildup of the methoxy- or hydroxycarbonyl adducts unlike the reactions seen for the unsubstituted cluster (see below).

The disubstituted cluster $Ru_3(CO)_{10}(P(OCH_3)_3)_2$ is even less reactive with base. No spectral changes were observed on standing overnight for a solution prepared from the disubstituted cluster in alkaline aqueous methanol ([base] = 0.2 M, 80/20 CH_3OH/H_2O, 25 °C), conditions under which both $Ru_3(CO)_{12}$ and $Ru_3(CO)_{11}(P(OCH_3)_3)$ reacted readily. However, in 96/2/2 (v/v/v) THF/CH_3OH0H_2O the disubstituted complex did undergo reaction with base (0.018 M) as evidenced by a shift over an hour's time of the absorption band λ_{max} at 415 nm (7.6×10^3 M^{-1} cm^{-1}) to 411 nm (8×10^3). The ^1H NMR of the isolated complex showed a hydride resonance split into a triplet centered at δ −12.35. The same properties have been noted for the product of the reaction of $HRu_3(CO)_{11}^-$ with 2 equiv of $P(OCH_3)_3$.[17] The trisubstituted cluster $Ru_3(CO)_9(P(OCH_3)_3)_3$ underwent no reaction observable spectrally when treated in a similar manner.

V. Kinetics of Hydroxide Reactions. Rates for reaction 19 in aqueous THF were determined by stopped-flow techniques. Plots of k_{obsd} (eq 5) vs. base were linear (slopes = k_2) with nonzero

(16) Ungermann, C.; Landis, V.; Moya, S. A.; Cohen, H.; Walker, H.; Pearson, R. G.; Rinker, R. G.; Ford, P. C. *J. Am. Chem. Soc.* **1979**, *101*, 5922.
(17) Taube, D.; Ford, P. C., work in progress.

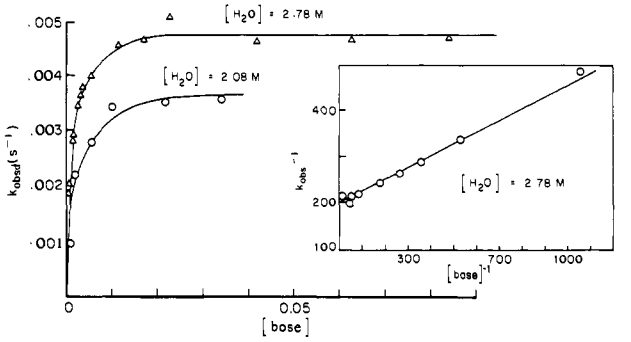

Figure 6. Plot of k_{obsd} vs. [base] for the formation of $HRu_3(CO)_{11}^-$ from $Ru_3(CO)_{12}$ plus $NaOCH_3$ in aqueous CH_3OH at two different concentrations of water (P_{CO} = 1.0 atm; T = 25 °C). Inset: Double reciprocal plot of k_{obsd}^{-1} vs. $[base]^{-1}$ for $[H_2O]$ = 2.78 M data.

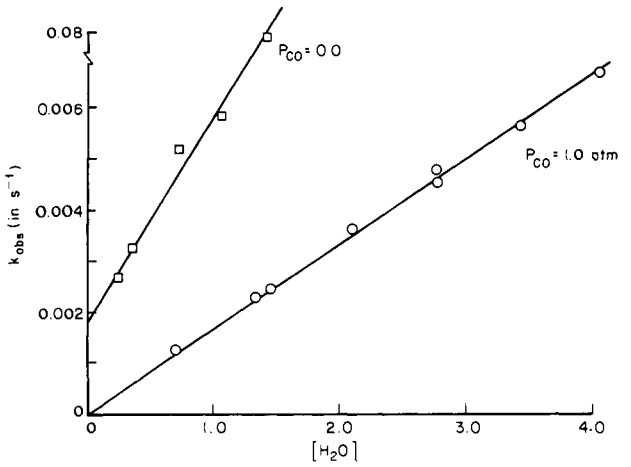

Figure 7. Plots of k_{obsd} vs. $[H_2O]$ for the formation of $HRu_3(CO)_{11}^-$ plus $NaOCH_3$ in aqueous CH_3OH ([base] = 0.045 M; T = 25.0 °C; CO plot is at P_{CO} = 1.0 atm; Ar plot is at P_{Ar} = 1 atm, P_{CO} = 0 atm).

intercepts (k_{-2}). For both KOH in 12.5/87.5 (v/v) H_2O/THF and $[(n\text{-}Bu)_4N]OH$ in 10/90 H_2O/THF, the k_2 values were about 1.2×10^3 M^{-1} s^{-1}, substantially less than k_1 for the reaction of $Ru_3(CO)_{12}$ with $NaOCH_3$ under similar conditions (Table III). The K_{eq}(kinetic) estimated from the k_2/k_{-2} ratio (the accuracy limited by uncertainty in k_{-2} values) lay in the range (1–10) × 10^3 M^{-1}, a value significantly lower than that for the analogous methoxycarbonyl formation.

Kinetics studies of hydride formation were carried out in aqueous methanol, a medium similar to that used for WGSR catalysis by ruthenium carbonyl.[2] Addition of $NaOCH_3$ to $Ru_3(CO)_{12}$ led to an immediate color change to give a spectrum virtually the same as that of $Ru_3(CO)_{11}(CO_2CH_3)^-$ followed by the slower formation of $HRu_3(CO)_{11}^-$ ion. Stopped-flow kinetics studies of the initial spectral change for the [base] range 0.001 to 0.02 M gave the second-order rate constant (1.8 ± 0.1) × 10^3 M^{-1} s^{-1}, very close to that for adduct formation in dry methanol (Table II). The slower hydride formation was studied by monitoring temporal absorbance changes at 460 nm on a conventional UV–vis spectrophotometer. In all cases plots of ln (abs(t) − abs(∞)) vs. t were linear, an indication that the rates of $HRu_3(CO)_{11}^-$ formation are first order in the total concentration of the Ru_3 reactant(s).

$$\frac{d[HRu_3(CO)_{11}^-]}{dt} = k_{obsd}[Ru_3] \quad (21)$$

The sensitivity of k_{obsd} to the variables $[H_2O]$, [base], and P_{CO} were investigated. Figure 6 displays the dependence of k_{obsd} on [base] for an aqueous methanol solution of $[H_2O]$ = 2.8 M. At low [base], k_{obsd} appears first order in base concentration, but at higher [base], it levels off to a constant value of 0.0047 s^{-1}. At constant [base] under 1 atm of P_{CO}, k_{obsd} increased linearly as $[H_2O]$ was varied from 0.25 to 4.0 M, giving slopes of 1.9×10^{-3}

M^{-1} s^{-1} at 0.065 M base and 1.7×10^{-3} M^{-1} s^{-1} at 0.045 M base (Figure 7). Under argon, a linear plot was also observed at 0.045 M [base] but the slope was larger (4.0×10^{-3} M^{-1} s^{-1}), and a nonzero intercept of about 3×10^{-3} s^{-1} was observed at $[H_2O] = 0.0$ M (Figure 7), suggesting that under these conditions another reaction may be contributing to the spectral changes in methanol. Lastly, when P_{CO} was varied over the range 0.05 to 1.53 atm with [base] (0.044 M) and $[H_2O]$ (1.39 M) held constant, k_{obsd} was found invariant (2.7 ± 0.4) $\times 10^{-3}$ s^{-1}, but at $P_{CO} = 0.00$ atm, a much larger value of (8 ± 1) $\times 10^{-3}$ s^{-1} was measured.

Discussion

I. Equilibria and Rates of Adduct Formation. The reactions of the nucleophiles CH_3O^-, OH^-, or other alkoxides RO^- with $Ru_3(CO)_{12}$ led in each case to spectral changes consistent with formation of the one-to-one adducts $Ru_3(CO)_{11}(CO_2R)^-$. Although all three $M_3(CO)_{12}$ clusters formed one-to-one adducts with CH_3O^- in methanol with similar K_{eq}'s, the iron adduct $Fe_3(CO)_{11}(CO_2CH_3)^-$, unlike A or the osmium analogue, underwent cluster fragmentation (eq 12) under CO and in the presence of $NaOCH_3$. This undoubtedly can be attributed to the weaker metal–metal bonding for the iron clusters.[18] Furthermore, the different stabilities toward fragmentation of the methoxycarbonyl clusters may explain the differences between iron and ruthenium in another homogeneous catalysis application, namely the disparate product distribution reported for the CO/H_2 reductive carbonylation of nitroaromatics when $Ru_3(CO)_{12}$ or $Fe_3(CO)_{12}$ were used as catalysts with methoxide as a cocatalyst in dry THF solution.[5c]

The reaction rates of the trinuclear clusters with $NaOCH_3$ in methanol followed the same order ($Fe_3(CO)_{12} > Ru_3(CO)_{12} > Os_3(CO)_{12}$) seen for the K_{eq} values. Comparison with the mononuclear pentacarbonyls shows a reversal, $Os(CO)_5 > Ru(CO)_5 > Fe(CO)_5$ (Table II). Notably, for ruthenium and osmium the rates for methoxycarbonyl formation were larger for the mononuclear complex than for the cluster; however, the opposite is the case for iron. One possible explanation for the higher reactivity of $Fe_3(CO)_{12}$ is the presence of bridging carbonyls,[19] a structural feature of $Fe_3(CO)_{12}$ but not of the Ru_3 or Os_3 analogues. Bridging carbonyls are more electron withdrawing than are terminal carbonyls,[20] thus they are more able to accommodate the charge developing on the cluster in the transition state. In this context, it is interesting to note that the tetranuclear iridium carbonyl $Ir_4(CO)_{12}$ undergoes significant structural rearrangement upon formation of a methoxycarbonyl adduct. The carbonyls of the parent compound are all terminally coordinated, but in the $Ir_4(CO)_{11}(CO_2CH_3)^-$ ion, three carbonyls are bridging.[12]

Darensbourg and Darensbourg[21] have previously examined the reactivity of the group 6 metal carbonyls with nucleophiles such as Grignard reagents. Those carbonyls having the higher vibrational force constants (i.e., the lesser π-back-bonding from the metal) were shown to be the more reactive. However, the unsubstituted carbonyl complexes of the iron triad show only a small range in their highest F_{CO} values.[22-26] Thus, other factors are likely to be at least equally influential to the kinetics, and reactivity orders may be the result of fortuitous combinations of such factors as variations in steric effects owing to different metal atom radii and coordination geometries, specific solvation, and metal–CO back-bonding as the metal center and nuclearity are changed.

For $RO^- = CH_3O^-$, the K_{eq} values for reaction of $Ru_3(CO)_{12}$ with $NaOH_3$ are markedly solvent dependent and range from 10^3 in methanol to 3×10^4 M^{-1} in 90/10 THF/CH_3OH (v/v). Furthermore, higher order adducts were seen in the mixed solvent. This suggests that the small anion CH_3O^- (and/or its ion pair $Na^+CH_3O^-$) is much more strongly solvated by the CH_3OH than by THF and that the destabilization of this species by increasing the THF concentration more than compensates for similar effects on the cluster adduct A (or its ion pair). Rates of the reaction of $NaOCH_3$ with $Ru_3(CO)_{12}$ are similarly solvent dependent and parallel the relative rates seen for $Fe(CO)_5$ under analogous conditions.[1a] We attribute these differences to the increases in the activity of $NaOCH_3$ as the percentage of dipolar, but aprotic, THF is raised at the expense of methanol in the solvent. A smaller but substantial solvent effect was also noted in the 90/10 *i*-PrOH/CH_3OH mixed solvent where k_1 was an order of magnitude larger than in methanol. Again methoxide is apparently less strongly solvated by the less acidic isopropyl alcohol. Measures of such anion solvation are the Gutmann acceptor numbers[27] which for THF, isopropyl alcohol, and methanol are 8, 18.3, and 33.5, respectively. This order is inverse to the reactivities of $NaOCH_3$ in these solvents, consistent with the argument that the more strongly accepting (anion solvating) media reduce the activity of $NaOCH_3$ toward adduct formation.

The studies in isopropyl alcohol also allowed comparisons of the reactivities of several oxyanions with $Ru_3(CO)_{12}$ and gave the order $CH_3O^- > OH^- > C_2H_5O^- > i\text{-}PrO^-$. Similar relative reactivities for methoxide and hydroxide were seen in THF solution (Table III) and are consistent with the generally observed greater nucleophilicity of the methoxide ion.[28] However, the lesser reactivities of ethoxide and isopropoxide, both of which are stronger Brønsted bases,[15] may reflect the influence of steric factors for these larger anions. Similar steric factors have been invoked to account for the relative rates of alkoxycarbonyl formation via the reaction of $PtCl(PPh_3)_2CO^+$ with various alcohols.[29]

The substituted clusters $Ru_3(CO)_{12-x}L_x$ ($L = P(OCH_3)_3$, $x = 1$, 2, or 3) were found to be much less reactive with $NaOCH_3$ as would be expected given the electron-donating nature of L relative to CO. For $x = 1$, adduct formation was not observable in methanol solution but could be detected in 50/50 THF/CH_3OH solutions with a K_{eq}(kinetic) value more than two orders of magnitude smaller than that for the unsubstituted cluster. Adduct formation is considerably less favored for the di- and trisubstituted clusters. As previous workers have noted,[1a,21,30] the replacement of one CO in a mononuclear complex by a more electron-donating ligand deactivates the remaining CO's toward reaction with nucleophiles. For the trinuclear clusters, the present data demonstrates that the rate of reaction with $NaOCH_3$ is 10^2 faster for $Ru_3(CO)_{12}$ than for $Ru_3(CO)_{11}P(OCH_3)_3$ in either 50/50 or 90/10 THF/CH_3OH. Given that, for the clusters, the nucleophile has the option of reacting with a CO on an unsubstituted metal, the lowered reactivity demonstrates the efficiency of the metal–metal bonds in transmitting electronic effects.

II. Formation of the Hydride. The reaction of $Ru_3(CO)_{12}$ with hydroxide leads first to adduct formation

$$Ru_3(CO)_{12} + OH^- \overset{K_2}{\rightleftharpoons} Ru_3(CO)_{11}(CO_2H)^- \qquad (22)$$

followed by decarboxylation to $HRu_3(CO)_{11}^-$. In aqueous methanol, an additional reaction is the "dead end" equilibrium formation of the methoxycarbonyl adduct.

$$Ru_3(CO)_{12} + CH_3O^- \overset{K_1}{\rightleftharpoons} Ru_3(CO)_{11}(CO_2CH_3)^- \qquad (23)$$

In this medium the relative concentrations of the relevant species are determined by the equilibrium constants K_1 and K_2, the concentration of base, and the partitioning of the methoxide and hydroxide according to the equilibrium

(18) Housecraft, C. E.; Wade, K.; Smith, B. C. *J. Chem. Soc., Chem. Commun.* **1978**, 765.
(19) Dahl, L. F.; Blount, C. *Inorg. Chem.* **1965**, *4*, 1373–5.
(20) Avanzino, S. C.; Jolly, W. L. *J. Am. Chem. Soc.* **1976**, *98*, 6505.
(21) Darensbourg, D. J.; Darensbourg, M. Y. *Inorg. Chem.* **1970**, *9*, 1691.
(22) Using the estimation method of Timney,[23] one calculates that F_{CO} values of the axial CO's for the $M_3(CO)_{12}$ and $M(CO)_5$ species to fall in the range 17.0 ± 0.1 mdyn/A. A somewhat broader range of values have been reported as the result of various calculations, i.e., $Ru_3(CO)_{12}$ (F_{CO} = 16.7 mdyn/A),[24] $Fe(CO)_5$ (17.0),[25] $Os_3(CO)_{12}$ (16.96,[25] 16.8[24]), but these values indicate no clear trends with k_1 values.
(23) Timney, J. A. *Inorg. Chem.* **1979**, *18*, 2502.
(24) Battiston, G. A.; Bor, G.; Dietler, V. K.; Kettle, S. F. A.; Rossetti, R.; Sbrignadello, G.; Stanghellini, P. L. *Inorg. Chem.* **1980**, *19*, 1961.
(25) Bor, G. *Inorg. Chim. Acta* **1969**, *3*, 191.
(26) Huggins, D. K.; Flitcoft, J.; Kaesz, H. D. *Inorg. Chem.* **1965**, *4*, 166.
(27) Gutmann, V. *Coord. Chem. Rev.* **1976**, *18*, 225.
(28) Bender, M. L.; Glasson, W. A. *J. Am. Chem. Soc.* **1959**, *81*, 1590.
(29) Byrd, J. E.; Halpern, J. *J. Am. Chem. Soc.* **1971**, *93*, 1634.
(30) Darensbourg, M. Y.; Condor, H. L.; Darensbourg, D. J.; Hasday, C. *J. Am. Chem. Soc.* **1973**, *95*, 5919.

$$CH_3O^- + H_2O \rightleftharpoons CH_3OH + OH^- \quad (24)$$

where

$$K_b = a(OH^-)/a(CH_3O^-)a(H_2O) = 0.0054\ M^{-1} \quad (25)$$

at 25 °C in methanol.[31] Over the range of $[H_2O]$ used here (0.25–4 M) more than 95% of the alkaline base is in the form of methoxide and $[OH^-]$ can be approximated as $K_b[H_2O][CH_3O^-]$.

The mechanisms of metal hydride formation from the reaction of metal carbonyls and base have been the subject of considerable speculation as well as some quantitative investigation. This discussion will focus on two potentially competing pathways which have been suggested for decarboxylation: (i) unimolecular "β-elimination" from the hydroxycarbonyl (eq 26) and (ii) prior deprotonation to give the carbon-bonded CO_2 complex (eq 27) followed by rate-limiting decarboxylation (eq 28)

$$Ru_3(CO)_{11}(CO_2H)^- \xrightarrow{k'} HRu_3(CO)_{11}^- + CO_2 \quad (26)$$

$$Ru_3(CO)_{11}(CO_2H)^- + B^- \rightleftharpoons BH + Ru_3(CO)_{11}(CO_2)^{2-} \quad (27)$$

$$Ru_3(CO)_{11}(CO_2)^{2-} \xrightarrow{k''} Ru_3(CO)_{11}^{2-} + CO_2 \quad (28)$$

$$Ru_3(CO)_{11}^{2-} + BH \xrightarrow{\text{fast}} HRu_3(CO)_{11}^- + B^- \quad (29)$$

where $B^- = CH_3O^-$ or OH^-. An alternative mechanism, reaction with hydroxide to give a carbon-coordinated carbonic acid complex followed by rate-limiting β-elimination of bicarbonate,[32] would have essentially the same kinetics as mechanism ii above.

It is assumed that the equilibria in eq 22, 23, 24, and 27 are rapidly established relative to the slower hydride formation reaction, the formation of $HRu_3(CO)_{11}^-$ via both eq 27 and 28 would have the following rate law

$$\frac{d[HRu_3(CO)_{11}^-]}{dt} = \frac{(k' + k''K_3[B^-])K_2K_b[H_2O][B^-][Ru_3]}{1 + K_1[B^-] + K_2K_b[B^-][H_2O] + K_3K_2K_b[H_2O][B^-]^2} \quad (30)$$

where $[Ru_3] = [A] + [Ru_3(CO)_{11}CO_2H^-] + [Ru_3(CO)_{12}] + [Ru_3(CO)_{11}(CO_2)^{2-}]$, and $[B^-] \cong [CH_3O^-]$.

Given that the electronic spectrum of the adduct mixture immediately after mixing $Ru_3(CO)_{12}$ with alkaline base in aqueous methanol is indistinguishable from that obtained from the reaction of $Ru_3(CO)_{12}$ with $NaOCH_3$ in anhydrous methanol, we conclude that the $K_3K_2K_b[B^-]^2[H_2O]$ term (formation of the $Ru_3(CO)_{11}(CO_2)^{2-}$ ion) is small relative to the other terms in the denominator of the rate expression. Furthermore, since $K_2 < K_1$ and $K_b[H_2O] \ll 1$, the $K_2K_b[B^-][H_2O]$ term must also be only a minor contributor to the overall denominator term for the concentrations of base and H_2O used for this investigation. Therefore, the rate expression can be simplified to

$$\frac{d[HRu_3(CO)_{11}^-]}{dt} = \frac{(k' + k''K_3[B^-])K_2K_b[H_2O][B^-][Ru_3]}{1 + K_1[B^-]} = k_{obsd}[Ru_3] \quad (31)$$

From eq 31 it can be seen that if eq 28 represented the predominant mechanism for the decarboxylation of $Ru_3(CO)_{11}(CO_2H)^-$ (i.e., $k''K_3[B^-] > k'$), then a plot of k_{obsd} vs. base concentration should be second order in $[B^-]$ at low concentration then become first order in $[B^-]$ at higher concentrations. This clearly is not the case observed in Figure 6, since k_{obsd} becomes zero order in $[B^-]$ at a relatively low concentration. Thus, we conclude that direct decarboxylation of the $Ru_3(CO)_{11}(CO_2)^{2-}$ dianion (eq 27 and 28) does not contribute significantly to the kinetics of $HRu_3(CO)_{11}^-$ formation. Similarly, the bicarbonate β-elimination mentioned above would not be consistent with the kinetic results indicated in Figure 6.

If the alternative pathway indicated by eq 26 (β-elimination of CO_2 from $Ru_3(CO)_{11}(CO_2H)^-$) represents the decarboxylation mechanism (i.e., $k' \gg k'K_3[B^-]$), then eq 31 can be further simplified to

$$M_3(CO)_{12} + CH_3O^- \underset{k_{-1}}{\overset{k_1}{\rightleftharpoons}} M_3(CO)_{11}(CO_2CH_3)^-$$

Notably, for this rate law, the dependence of k_{obsd} on $[B^-]$ should be first order at low concentrations leveling off to zero order at high $[B^-]$ as seen in Figure 6 and should be first order in $[H_2O]$ as seen in Figure 7. We have reached a similar conclusion with regard to the formation of the iron hydride $HFe(CO)_4^-$ via the reaction of $Fe(CO)_5$ plus hydroxide A, in the mixed solvent 50/48/2 THF/CH_3OH/H_2O (v/v/v), i.e., that the reaction occurs via decarboxylation of the hydroxycarbonyl adduct $Fe(CO)_4(CO_2H)^-$ rather than of the $Fe(CO)_4(CO_2)^{2-}$ dianion.[1]

A more quantitative evaluation of the data in Figures 6 and 7 provides some further confirmation of the validity of the above model. Double reciprocal plots of the data in Figure 6 are linear with slopes = $1/(k'K_2K_b[H_2O])$ and nonzero intercepts $K_1/k'K_2K_b[H_2O]$. Slope values of 0.38 ± 0.03 and 0.26 ± 0.02 M s and intercepts of 285 ± 10 and 205 ± 10 s were obtained for $[H_2O]$ = 2.08 and 2.78 M, respectively. According to eq 32 the intercept/slope ratio is K_1 and the average value $(8 \pm 1) \times 10^2$ M^{-1} is calculated for these two conditions. Although somewhat low, this value is quite comparable to the K_1 values measured by kinetic and static spectral methods for the formation of $Ru_3(CO)_{11}(CO_2CH_3)^-$ in neat methanol (Table II). Using this K_1 and K_b = 0.0054 M^{-1} and the respective concentrations, one can calculate the product $k'K_2$ from the slopes of the double reciprocal plots. The average value of $k'K_2 = (2.5 \pm 0.2) \times 10^2$ is thus obtained under a CO blanket (1.0 atm). For the k_{obsd} vs. $[H_2O]$ plot at constant $[B^-]$, Figure 7, the slope should (according to eq 32) equal $k'K_2K_b[B^-]/(1 + K_1[B^-])$. From the measured slope = 1.7 ± 0.1 M^{-1} s^{-1} plus the values $[B^-]$ = 0.045 M, $K_1 = 8 \times 10^2$ M, and K_b = 0.0054 M^{-1}, $k'K_2$ was calculated as $(2.6 \pm 0.2) \times 10^2$ M^{-1} s^{-1} for P_{CO} = 1.0 atm, in excellent agreement with the values of the $k'K_2$ product calculated from the independent Figure 6 data.

However, a much higher value of $k'K_2$ (about 1.2×10^3 M^{-1} s^{-1}) was obtained from the slope of the k_{obsd} vs. $[H_2O]$ plot measured under an argon atmosphere. Furthermore, the apparent nonzero intercept of this plot suggests that under these conditions the complex undergoes another reaction leading to spectral changes even in the absence of water. Although we have not yet evaluated this reaction in quantitative detail, a logical explanation is the labilization of CO from the $Ru_3(CO)_{11}(CO_2CH_3)^-$ ion and rearrangement to give the bridging methoxycarbonyl complex $Ru_3(CO)_{10}(\mu\text{-}CO_2CH_3)^-$ noted in the Results. Recent ligand substitution kinetics studies in these laboratories[33] have quantitatively confirmed the greatly enhanced lability of the $Ru_3(CO)_{11}(CO_2CH_3)^-$ ion (relative to $Ru_3(CO)_{12}$).

Similar enhanced lability might be expected for $Ru_3(CO)_{11}(CO_2H)^-$

$$Ru_3(CO)_{12-n}L_n + RO^- \underset{k_{-1}}{\overset{k_1}{\rightleftharpoons}} Ru_3(CO)_{11-n}L_n(CO_2R)^-$$

The resulting open coordination site might serve as the acceptor for the hydride in a concerted elimination of the CO_2 from the hydroxycarbonyl, thus explaining the faster rates for hydride formation under argon than under CO at 1 atm. However, the observation that a CO blanket even at 0.05 atm suppresses the hydride formation (by a factor of more than three) to a rate comparable to that seen under P_{CO} = 1.5 atm suggests two important conclusions. First, the equilibrium constant for eq 13 must be small, and dissociation is largely suppressed by low concentration of CO. Second, there must be a slower pathway for concerted CO_2 elimination from the $Ru_3(CO)_{11}(CO_2H)^-$ cluster not requiring CO dissociation. It is decarboxylation via this pathway which the kinetic studies at P_{CO} = 1.0 atm are evaluating.

(31) (a) Moore, J. W.; Pearson, R. G. "Kinetics and Mechanism", 3rd ed.; Wiley-Interscience: New York, 1981; p 361. (b) This value of K_b is calculated on the basis of the approximation that $a(CH_3OH)$ = 24.0 M.

(32) Darensbourg, D. J.; Rokicki, A. *Organometallics* **1982**, *1*, 1685.

Scheme I. Hypothetical Cycle for the Homogeneous WGSR Catalysis

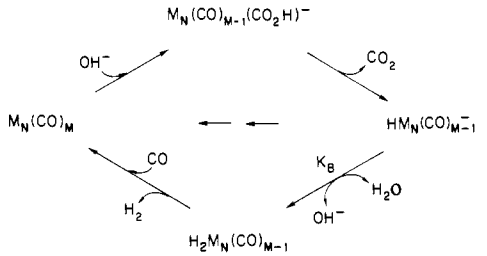

Notably, these are also the types of conditions used in the homogeneous catalysis of the water gas shift reaction.

III. Application to Shift Reaction Catalysis Cycles. Scheme I is a hypothetical catalysis cycle incorporating eq 1 and 2. In the context of this cycle and of the data presented above and previously, we will consider the catalysis by three different carbonyls: $Ru_3(CO)_{12}$, $Fe(CO)_5$, and $Ru(CO)_5$. The former two were among the first homogeneous WGSR catalysts described.[3a]

For the $Ru_3(CO)_{12}$-based catalyst, various studies[34] suggest that the principal catalytic cycle under mild conditions (about 100 °C, about 1 atm of P_{CO}) involves trinuclear clusters. The rate-limiting step in the catalysis is the conversion of $HRu_3(CO)_{11}^-$ back to $Ru_3(CO)_{12}$ and the resultant production of H_2. The $HRu_3(CO)_{11}^-$ ion can be protonated in strong acid to give H_2[16] and $Ru_3(CO)_{12}$ under CO but is an exceedingly weak base,[35] and such a pathway is precluded in the alkaline conditions (pH 9) of the mature WGSR catalyst. The catalysis is first order in P_{CO}, and we have proposed[16] a rate-limiting step involving addition of CO to the $HRu_3(CO)_{11}^-$ cluster followed by removal of hydride by reaction with H_2O to give H_2 by a mechanism yet to be delineated. The important point is that formation of $HRu_3(CO)_{11}^-$ occurs readily in solution, yet the very low basicity of this ion forces the ruthenium cluster to undergo a mechanistic path other than that shown in the lower half of Scheme I to close the cycle.

The catalysis by $Fe(CO)_5$ is limited in two ways. The equilibrium constant for the formation of the hydroxycarbonyl adduct $Fe(CO)_4(CO_2H)^-$ is several orders of magnitude smaller in aqueous alcohol than that for the ruthenium cluster and at least an order of magnitude smaller than that for the mononuclear ruthenium analogue. As a consequence, the formation of the hydride $HFe(CO)_4^-$ from $Fe(CO)_5$ plus base becomes rate limiting in the carbonate/bicarbonate buffered catalyst solutions. Raising the pH to accelerate this reaction would be unproductive given that the hydride anion is a relatively weak base and the formation of H_2 from $HFe(CO)_4^-$ would then become rate limiting under such conditions.[6c]

Several observations from this laboratory with regard to mononuclear ruthenium carbonyls also rationalize the report[36] that the WGSR activity of a ruthenium-based catalyst is quite high (in turnover number) when the catalysis is carried out in aqueous amine solutions at elevated temperatures and high P_{CO} (>50 atm) as well as at much lower ruthenium concentrations ($<10^{-4}$ M) than described above for the cluster ruthenium catalyst. Under these conditions, the ruthenium carbonyls are mononuclear, and even once the more forcing conditions are accounted for, it appears that the system based on mononuclear ruthenium complexes is more active than that based on trinuclear ruthenium or mononuclear iron catalysts. The kinetics data are consistent with this observation. Nucleophilic activation of $Ru(CO)_5$ with OH^- to give the hydroxycarbonyl has a much larger K_2 value than that for $Fe(CO)_5$, thus, as for the ruthenium clusters, formation of the hydride $HRu(CO)_4^-$ occurs quite readily in alkaline aqueous alcohol solutions. Furthermore, although the quantitative pK_a values for this anion have not been determined, indirect evidence[37] points to it being a stronger base than is $HFe(CO)_4^-$ and a much stronger base than is $HRu_3(CO)_{11}^-$. Thus $H_2Ru(CO)_4$ should readily form and undergo reductive elimination of H_2 under the catalyst conditions. Given these differences the mononuclear ruthenium species should indeed be the most active of the three catalysts.[38]

Acknowledgment. This research was supported by the U.S. Department of Energy, Office of Basic Energy Sciences. Ruthenium used in these investigations was provided on loan by Johnson-Matthey, Inc. Preliminary experiments with the $Ru_3(CO)_{12}$ cluster were carried out by Dr. Haim Cohen.

(33) Anstock, M.; Taube, D.; Gross, D. C.; Ford, P. C. *J. Am. Chem. Soc.* **1984**, *106*, 3696.
(34) Bricker, J. C.; Nagel, C. C.; Shore, S. G. *J. Am. Chem. Soc.* **1982**, *104*, 1444. A catalysis cycle based on trinuclear species was also proposed in ref 16.
(35) Keister, J. B. *J. Organomet. Chem.* **1980**, *190*, C36.
(36) Slegeir, W. A. R.; Sapienza, R. S.; Easterling, B. *ACS Symp. Ser.* **1981**, *152*, 325.
(37) Walker, H. W.; Pearson, R. G.; Ford, P. C. *J. Am. Chem. Soc.* **1983**, *105*, 1179–86.
(38) In this context it has been reported (Bricker, J. C.; Bhattacharyya, N.; Shore, S. G. *Organometallics* **1984**, *3*, 201) that in alkaline solution a WGSR catalyst prepared from $HOs(CO)_4^-$ has a higher initial activity than one prepared with use of $Os_3(CO)_{12}$ as the catalyst precursor.